Title
Elastic wave scattering and dynamic stress concentrations in exponential graded materials with two elliptic holes

Journal
Wave Motion, 51(3)

ISSN
0165-2125

Authors
Zhou, Chuanping
Hu, Chao
Ma, Fai
et al.

Publication Date
2014-04-01

DOI
10.1016/j.wavemoti.2013.11.005

Peer reviewed

Wave Motion 51 (2014) 466–475

Contents lists available at ScienceDirect

Wave Motion

journal homepage: www.elsevier.com/locate/wavemoti

Elastic wave scattering and dynamic stress concentrations in exponential graded materials with two elliptic holes

Chuanping Zhou [a,*], Chao Hu [a,b], Fai Ma [c], Diankui Liu [d]

[a] School of Aerospace Engineering and Applied Mechanics, Tongji University, Shanghai, 200092, China
[b] College of Civil Science and Engineering, Yangzhou University, Yangzhou, 225127, China
[c] College of Engineering, University of California, Berkeley, 94720, USA
[d] College of Aerospace and Civil Engineering, Harbin Engineering University, Harbin, 150001, China

HIGHLIGHTS

- FGMs used in this paper are developing materials other than traditional materials.
- Solving the elastic wave problem for two scattered bodies becomes complex.
- In especial, the scattered bodies studied are non-circular.
- The complex function method used in elastodynamics is another bright spot.

ARTICLE INFO

Article history:
Received 27 January 2013
Received in revised form 16 October 2013
Accepted 2 November 2013
Available online 26 November 2013

Keywords:
Elastic waves scattering
Dynamic stress concentrations
Conformal mapping methods
Local coordinate system
Graded materials
Two elliptic holes

ABSTRACT

Based on the elastodynamics, employing complex functions and conformal mapping methods, and local coordinates, the scattering of elastic waves and dynamic stress concentrations in infinite exponential graded materials with two holes are investigated. A general solution of the problem and expression satisfying the given boundary conditions are derived. The problem can be reduced to the solution of an infinite system of algebraic equations. As an example, numerical results of dynamic stress concentration factors for two elliptic holes in exponential graded materials are presented, and the influence of incident wave number and holes spacing on dynamic stress distributions is analyzed.

1. Introduction

Elastic wave methods can be used to describe and simulate the stress strain states which are produced by a variety of dynamic loads in solid media or structures. The elastic wave propagation, scattering and dynamic stress concentration, as well as the localization of vibration in structures with cutouts are important frontier problems in the realm of mechanics. The investigations on these problems can promote the innovation and development of classic structural dynamics and their solving methods.

Nowadays functionally graded materials have been widely used in aviation, aerospace, shipping and mechanical engineering. Stress analysis and strength designs of structures are crucial to structure designs. To meet the requirements of engineering designs, it is unavoidable to make holes in functionally graded materials. Holes bring about stress

* Corresponding author. Tel.: +86 18817598209.
E-mail addresses: joany0204@hotmail.com, zhouchuanping@126.com (C. Zhou).

0165-2125/$ – see front matter © 2013 Elsevier B.V. All rights reserved.
http://dx.doi.org/10.1016/j.wavemoti.2013.11.005

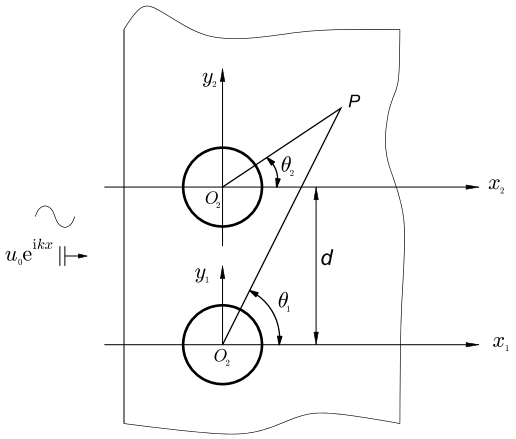

Fig. 1. Schematic of the incident of elastic waves in infinite graded materials.

concentrations, especially dynamic stress concentrations, which will reduce the loading capacity and life time of the structures. Therefore, the study on the scattering of elastic waves and dynamic stress concentrations in graded materials with holes is an important project.

The single circular hole is one of the most simple research models, which Pao and Maw [1,2] made exhaustive discussions. Complex function method proposed by Muskhelishvili [3] is applied to the elastostatics problems in two dimensions with the noncircular holes, which is considered a groundbreaking work. Thereafter, the complex function method developed by Liu et al. [4] is applied to the elastodynamics problems in two dimensions with the arbitrary shape holes. Li et al. [5] worked out at the dynamic stress intensity factor of a cylindrical interface crack in functionally graded materials by means of Fourier transform methods. Numerical methods are widely used in modern elastodynamics researches. Liu et al. [6,7] investigated the transient response of an embedded crack and edge crack perpendicular to the boundary of an orthotropic functionally graded strip. S. Ueda [8] discussed the surface crack problem for a layered plate with a functionally graded non-homogeneous interface. Ma et al. [9] studied the dynamic behavior of a finite crack in functionally graded materials subjected to the normally incident elastic harmonic waves. Fang et al. [10] made a research on the dynamic stress of a circular cavity buried in a semi-infinite functionally graded material subjected to shear waves. C.H. Daros [11] used the boundary element method to study SH-waves in a class of inhomogeneous anisotropic media and presented numerical results. Recently, P.A. Martin [12] investigated the scattering by defects in an exponentially graded layer and Q. Yang et al. [13,14] discussed stress analysis of a functional graded material plate with a circular hole.

Based on the theory of elastic wave [15,16], we discuss the scattering of elastic waves and dynamic stress concentrations by two holes in exponential graded materials. By using the complex function method and local coordinate system, the solutions of this problem under the influence of incident waves with different wave numbers are obtained. Then a solution of the problem can be reduced to the solution of the infinite system of algebraic equations. At last, the numerical results of dynamic stress concentration factors around two stress-free elliptic holes in exponential graded materials are presented and discussed.

2. Equation of wave motion and its solution

Consider the infinite exponential graded materials in which the shear modulus and density change continuously along with the x direction with the variation form as

$$\mu(x) = \mu_0 \exp(2\beta x), \qquad \rho(x) = \rho_0 \exp(2\beta x) \tag{1}$$

where μ_0, ρ_0 are the shear modulus and density at $x = 0$, and β is the non-homogeneous coefficient which stands for the spatial variation of the shear modulus and density in exponential graded materials.

The incidence of anti-plate shear waves along the x direction is considered in infinite exponential graded materials with two holes depicted in Fig. 1. We can express the governing equation of elastic wave motions in exponential graded materials as

$$\frac{\partial \tau_{xz}}{\partial x} + \frac{\partial \tau_{yz}}{\partial y} = \rho(x)\frac{\partial^2 u}{\partial t^2} \tag{2}$$

in which τ_{xz}, τ_{yz} are the shear stress.

We can write the constitutive relation for the anti-plane shear deformation

$$\tau_{xz} = \mu(x)\frac{\partial u}{\partial x}, \qquad \tau_{yz} = \mu(x)\frac{\partial u}{\partial y}. \tag{3}$$

Substituting Eq. (3) into the Eq. (2), we can derive the resulting equation in the form

$$\frac{\partial^2 u}{\partial x^2}+\frac{\partial^2 u}{\partial y^2}+2\beta\frac{\partial u}{\partial x}=\frac{1}{c_s^2}\frac{\partial^2 u}{\partial t^2} \tag{4}$$

where $c_s=\sqrt{\mu_0/\rho_0}$ is the velocity of shear waves.

Let $u=U\exp(-\mathrm{i}\omega t)$, and the Eq. (4) is expressed into the following form

$$\nabla^2 U+2\beta\frac{\partial U}{\partial x}+k^2U=0 \tag{5}$$

where ω is the angular frequency of incident waves, $k=\omega/c_s$ is the wave number.

Suppose that a solution of Eq. (5) is

$$U=\exp(-\beta x)w\,(x,y) \tag{6}$$

in which $w(x,y)$ is the derived functions.

Substituting Eq. (6) into Eq. (5), we note that $w(x,y)$ needs to satisfy the following equation

$$\nabla^2 w+\alpha^2 w=0 \tag{7}$$

with $\alpha=\sqrt{k^2-\beta^2}$. When the frequency of the incident wave is smaller than the non-homogeneous coefficient, the solution presents a simple vibration with decreasing amplitude. In this paper, we discard this situation, so here, we set $\beta^2<k^2$.

Now we consider the complex function method and introduce the complex variable $z=x+\mathrm{i}y$, $\bar{z}=x-\mathrm{i}y$.

By using Eqs. (5)–(7), we can obtain the elastic waves $U\exp(-\mathrm{i}\omega t)=u_0\exp(-\beta x)\exp(\mathrm{i}\alpha x-\mathrm{i}\omega t)$.

Recall that Eq. (5) determine the scattered wave from holes in the exponential graded materials, and we can express the solution of the scattered field as

$$u^{(s)}=\exp\left[-\beta\mathrm{Re}(z)\right]\sum_{n=-\infty}^{\infty}A_nH_n^{(1)}(\alpha|z|)\left\{\frac{z}{|z|}\right\}^n\exp(-\mathrm{i}\omega t) \tag{8}$$

where $H_n^{(1)}(\cdot)$ is the nth Hankel function of the first kind and A_n are mode coefficients of scattered waves which may be determined by the given boundary conditions.

3. Excitation of incident waves and total wave field

Considering exponential graded materials under the influence of anti-plate shear waves and omitting the time factor $\exp(-\mathrm{i}\omega t)$ from here on, we represent the incident waves by an infinite series

$$u^{(i)}=u_0\exp(-\beta x)\exp(\mathrm{i}\alpha x)=u_0\exp[-\beta\mathrm{Re}(z)]\sum_{n=-\infty}^{\infty}i^nJ_n(\alpha|z|)\left\{\frac{z}{|z|}\right\}^n \tag{9}$$

in which u_0 is the amplitude of the incident waves and α is the wave number of the propagating waves.

We can also write the form of the scattered field as

$$u^{(s)}=\exp[-\beta\mathrm{Re}(z)]\sum_{n=-\infty}^{\infty}A_nH_n^{(1)}(\alpha|z|)\left\{\frac{z}{|z|}\right\}^n. \tag{10}$$

When the multiple scattering between each hole is considered, the scattering of elastic waves by the two holes can be expressed as

$$u_m^{(s)}=\sum_{n=-\infty}^{\infty}A_n^mH_n^{(1)}\,(\alpha r)\exp(\mathrm{i}n\varphi) \tag{11}$$

where $m=1,2$; A_n^m are mode coefficients of scattered waves which are produced by the mth hole.

Hence, the total wave field of elastic waves in exponential graded materials is produced by the superposition of the incident field and the scattered field by the two holes, i.e.,

$$u^{(t)}=u^{(i)}+u_m^{(s)}. \tag{12}$$

Without loss of generality, we investigate two stress-free holes with boundary condition

$$\tau_{\rho z}^m|_{\rho=a}=0. \tag{13}$$

4. Determination of mode coefficients and dynamic stress concentration

A hole of arbitrary shape (with a smooth boundary) in the z plane may be mapped into a unit circle in the ζ plane by the mapping function $z=\Omega(\zeta)$ to satisfy the given boundary condition of noncircular hole. The conformal mapping function

can be taken as

$$z = \Omega(\zeta) = R\left(\zeta + \sum_{l=1}^{\infty} C_l \zeta^{-l}\right). \tag{14}$$

Here R is a positive constant and C_l are complex constants.

Elliptic holes are investigated with mapping function as

$$z = \Omega(\zeta) = \frac{a}{1+c}\left(\zeta + \frac{c}{\zeta}\right), \quad \zeta = \rho\exp(\mathrm{i}\theta) \tag{15}$$

where c is the eccentricity ratio of ellipse.

Substituting Eqs. (12) and (15) into the boundary condition of the noncircular holes Eq. (13) and employing the local coordinate system method, we obtain an infinite system of algebraic equations which can determine the mode coefficients A_n^1, A_n^2

$$\sum_{n=-\infty}^{\infty} E_n X_n = E, \tag{16}$$

where

$$E_n = \begin{bmatrix} E_n^{11} & E_n^{12} \\ E_n^{21} & E_n^{22} \end{bmatrix} \qquad X = \begin{bmatrix} A_n^1 \\ A_n^2 \end{bmatrix} \qquad E = \begin{bmatrix} E^1 \\ E^2 \end{bmatrix}$$

$$E^j = \frac{1}{\rho_j \Omega'(\zeta_j)} u_0 \exp\left\{(\mathrm{i}\alpha - \beta)\,\mathrm{Re}\left[\Omega(\zeta_j)\right]\right\}(\beta - \mathrm{i}\alpha)\,\mathrm{Re}\left[\zeta_j \Omega'(\zeta_j)\right] \quad (j = 1, 2)$$

$$\begin{aligned} E_n^{11} &= \frac{1}{\rho_1 \Omega'(\zeta_1)} \exp\left[-\beta \mathrm{Re}(\Omega(\zeta_1))\right] \left\{ H_n^{(1)}(\alpha|\Omega_1(\zeta_1)|)\left[-\beta \mathrm{Re}(\zeta_1 \Omega'(\zeta_1)) + \mathrm{i}n\mathrm{Im}\left(\zeta_1 \frac{\Omega'(\zeta_1)}{\Omega(\zeta_1)}\right)\right] \right. \\ &\quad \left. + \frac{\alpha}{2}\left[H_{n-1}^{(1)}(\alpha|\Omega(\zeta_1)|) - H_{n+1}^{(1)}(\alpha|\Omega(\zeta_1)|)\right] \mathrm{Re}\left(\zeta_1 \frac{\overline{\Omega(\zeta_1)}}{|\Omega(\zeta_1)_1|}\Omega'(\zeta_1)\right)\right\} \left\{\frac{\Omega(\zeta_1)}{|\Omega(\zeta_1)|}\right\}^n \\ E_n^{12} &= \frac{1}{\rho_2 \Omega'(\tilde{\zeta}_2)} \exp\left[-\beta \mathrm{Re}(\Omega(\tilde{\zeta}_2))\right] \left\{ H_n^{(1)}\left(\alpha|\Omega(\tilde{\zeta}_2)|\right)\left[-\beta \mathrm{Re}(\tilde{\zeta}_2 \Omega'(\tilde{\zeta}_2)) + \mathrm{i}n\mathrm{Im}\left(\tilde{\zeta}_2 \frac{\Omega'(\tilde{\zeta}_2)}{\Omega(\tilde{\zeta}_2)}\right)\right] \right. \\ &\quad \left. + \frac{\alpha}{2}\left[H_{n-1}^{(1)}(\alpha|\Omega(\tilde{\zeta}_2)|) - H_{n+1}^{(1)}(\alpha|\Omega(\tilde{\zeta}_2)|)\right] \mathrm{Re}\left(\tilde{\zeta}_2 \frac{\overline{\Omega(\tilde{\zeta}_2)}}{|\Omega(\tilde{\zeta}_2)|}\Omega'(\tilde{\zeta}_2)\right)\right\} \left\{\frac{\Omega(\tilde{\zeta}_2)}{|\Omega(\tilde{\zeta}_2)|}\right\}^n \\ E_n^{21} &= \frac{1}{\rho_1 \Omega'(\tilde{\zeta}_1)} \exp\left[-\beta \mathrm{Re}(\Omega(\tilde{\zeta}_1))\right] \left\{ H_n^{(1)}(\alpha|\Omega(\tilde{\zeta}_1)|)\left[-\beta \mathrm{Re}(\tilde{\zeta}_1 \Omega'(\tilde{\zeta}_1)) + \mathrm{i}n\mathrm{Im}\left(\tilde{\zeta}_1 \frac{\Omega'(\tilde{\zeta}_1)}{\Omega(\tilde{\zeta}_1)}\right)\right] \right. \\ &\quad \left. + \frac{\alpha}{2}\left[H_{n-1}^{(1)}(\alpha|\Omega(\tilde{\zeta}_1)|) - H_{n+1}^{(1)}(\alpha|\Omega(\tilde{\zeta}_1)|)\right] \mathrm{Re}\left(\tilde{\zeta}_1 \frac{\overline{\Omega(\tilde{\zeta}_1)}}{|\Omega(\tilde{\zeta}_1)|}\Omega'(\tilde{\zeta}_1)\right)\right\} \left\{\frac{\Omega(\tilde{\zeta}_1)}{|\Omega(\tilde{\zeta}_1)|}\right\}^n \\ E_n^{22} &= \frac{1}{\rho_2 \Omega'(\zeta_2)} \exp\left[-\beta \mathrm{Re}(\Omega(\zeta_2))\right] \left\{ H_n^{(1)}(\alpha|\Omega(\zeta_2)|)\left[-\beta \mathrm{Re}(\zeta_2 \Omega'(\zeta_2)) + \mathrm{i}n\mathrm{Im}\left(\zeta_2 \frac{\Omega'(\zeta_2)}{\Omega(\zeta_2)}\right)\right] \right. \\ &\quad \left. + \frac{\alpha}{2}\left[H_{n-1}^{(1)}(\alpha|\Omega(\zeta_2)|) - H_{n+1}^{(1)}(\alpha|\Omega(\zeta_2)|)\right] \mathrm{Re}\left(\zeta_2 \frac{\overline{\Omega(\zeta_2)}}{|\Omega(\zeta_2)|}\Omega'(\zeta_2)\right)\right\} \left\{\frac{\Omega'(\zeta_2)}{|\Omega(\zeta_2)|}\right\}^n \end{aligned}$$

$$\zeta_1 = a\exp(\mathrm{i}\theta_1), \qquad z_1 = \frac{a}{1+c}\left(\zeta_1 + \frac{c}{\zeta_1}\right)$$

$$\tilde{\zeta}_2 = \sqrt{a^2 + d^2 + 2ad\sin\theta_1}\exp\left(\mathrm{i}\arccos\frac{a\cos\theta_1}{\sqrt{a^2 + d^2 + 2ad\sin\theta_1}}\right),$$

$$\tilde{z}_2 = \frac{a}{1+c}\left(\zeta_2 + \frac{c}{\zeta_2}\right)$$

$$\zeta_2 = a\exp(\mathrm{i}\theta_2), \qquad z_2 = \frac{a}{1+c}\left(\zeta_2 + \frac{c}{\zeta_2}\right)$$

$$\tilde{\zeta}_1 = \sqrt{a^2 + d^2 - 2ad\sin\theta_2}\exp\left(-\mathrm{i}\arccos\frac{a\cos\theta_2}{\sqrt{a^2 + d^2 - 2ad\sin\theta_2}}\right), \qquad \tilde{z}_1 = \frac{a}{1+c}\left(\zeta_1 + \frac{c}{\zeta_1}\right).$$

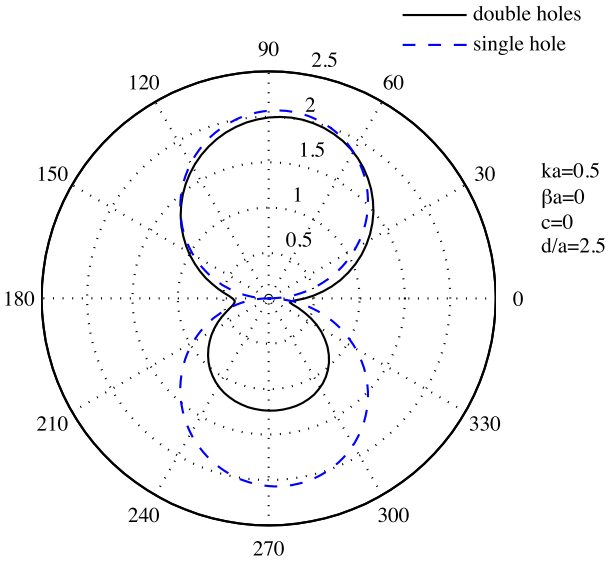

Fig. 2. Dynamic stress around single holes versus two circular holes $ka = 0.5$, $\beta a = 0$, $d/a = 2.5$.

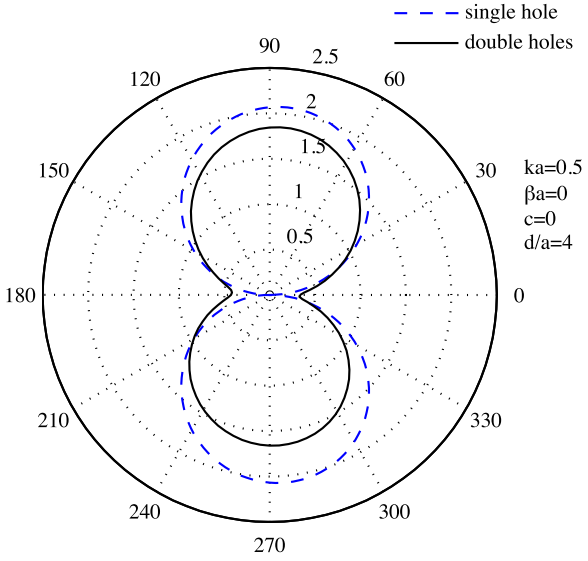

Fig. 3. Dynamic stress around single holes versus two circular holes $ka = 0.5$, $\beta a = 0$, $d/a = 4.0$.

Multiplying by $\exp(-is\theta_j)$ on both sides of Eq. (16) and integrating from $-\pi$ to π, we write the infinite algebraic equations which determine mode coefficients A_n^1, A_n^2 as

$$\sum_{-\infty}^{\infty} E_{ns} X_n = E_s \tag{17}$$

where $E_{ns} = \frac{1}{2\pi}\int_{-\pi}^{\pi} E_n \exp\left(-is\theta_j\right) d\theta_j$, $E_s = \frac{1}{2\pi}\int_{-\pi}^{\pi} E \exp\left(-is\theta_j\right) d\theta_j$.

The dynamic stress concentration is defined as the ratio of stress due to the total wave at a point to the stress due to the incident waves (without the holes) at the same points [1]. In terms of the definition, the dynamic stress concentration factor for holes in exponential graded materials can be described as

$$\tau_{\theta z}^{*} = \left|\frac{\tau_{\theta z}}{\tau_0}\right| \tag{18}$$

where $\tau_{\theta z}^{*}$ is dimensionless stress representing the dynamic stress concentration factor and $\tau_0 = \mu\kappa u_0$ is the amplitude of the incident waves.

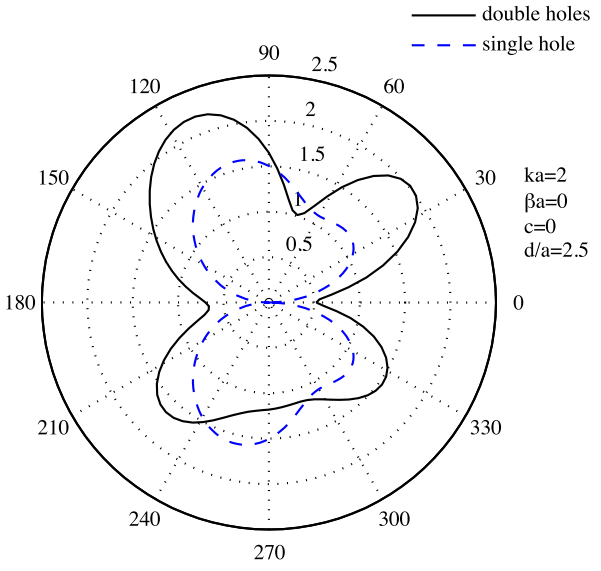

Fig. 4. Dynamic stress around single holes versus two circular holes $ka = 2.0$, $\beta a = 0$, $d/a = 2.5$.

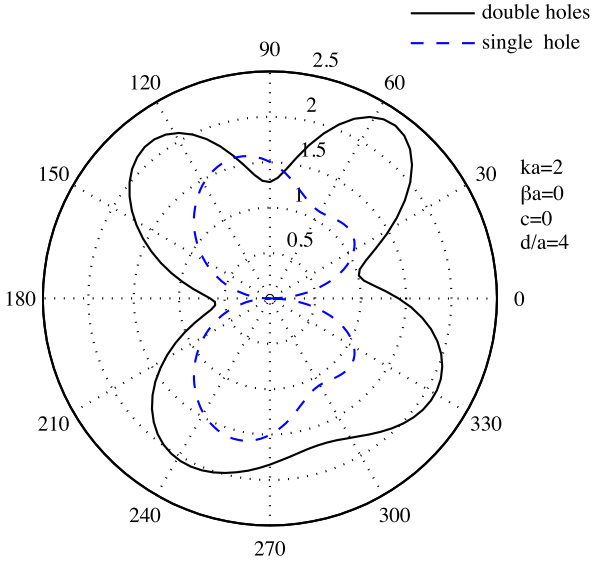

Fig. 5. Dynamic stress around single holes versus two circular holes $ka = 2.0$, $\beta a = 0$, $d/a = 4.0$.

Eq. (18) gives the dynamic stress concentration factor near the jth hole as the form

$$\begin{aligned}\mathrm{DSCF}_j = {} & \frac{1}{\alpha}\frac{1}{\rho_j \Omega'(\zeta_j)} \exp\left[(-\beta + \mathrm{i}\alpha)\mathrm{Re}(\Omega(\zeta_j))\right](\beta - \mathrm{i}\alpha)\mathrm{Im}\left[\zeta_j \Omega'(\zeta_j)\right] \\ & + \frac{1}{\alpha u_0}\sum_{m=1}^{2}\frac{1}{\rho_m \Omega'(\zeta_m)} \exp\left[-\beta \mathrm{Re}(\Omega(\zeta_m))\right] \\ & \times \sum_{n=-\infty}^{\infty} A_n^m \left\{ \left[\beta \mathrm{Im}(\zeta_m \Omega'(\zeta_m)) + \mathrm{i}n\mathrm{Re}\left(\zeta_m \frac{\Omega'(\zeta_m)}{\Omega(\zeta_m)}\right)\right] H_n^{(1)}(\alpha|\Omega(\zeta_m)|) \right. \\ & \left. - \frac{\alpha}{2}\mathrm{Im}\left(\zeta_m \frac{\overline{\Omega(\zeta_m)}}{|\Omega(\zeta_m)|}\Omega'(\zeta_m)\right)\left[H_{n-1}^{(1)}(\alpha|\Omega(\zeta_m)|) - H_{n+1}^{(1)}(\alpha|\Omega(\zeta_m)|)\right]\right\}\left\{\frac{\Omega(\zeta_m)}{|\Omega(\zeta_m)|}\right\}^n. \end{aligned} \tag{19}$$

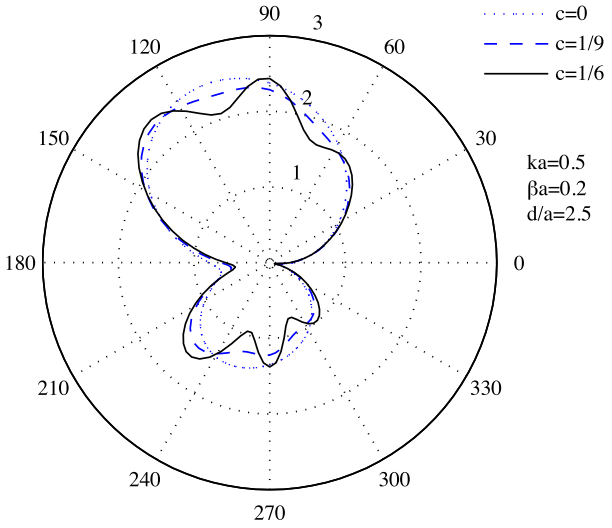

Fig. 6. Distributions of dynamic stress concentrations around two elliptic holes $ka = 0.5$, $\beta a = 0.2$, $d/a = 2.5$.

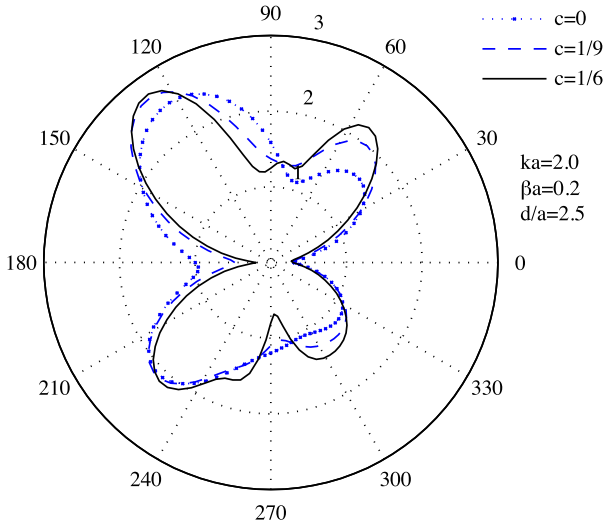

Fig. 7. Distributions of dynamic stress concentrations around two elliptic holes $ka = 2.0$, $\beta a = 0.2$, $d/a = 2.5$.

5. Numerical examples and discussions

Calculation programs of dynamic stress concentration around the opening are prepared and the dynamic stress distribution curves are plotted. For the numerical calculation, set Poisson ratio $\nu = 0.3$, term number of the series $n = 10$–20. All the figures below illuminate the upper hole of the two with layout from top to bottom. The hole-spacing is d.

As Figs. 2–5 are mentioned, we describe the hoop angular distributions of dynamic stress around the upper circular holes in homogeneous materials (i.e., $\beta = 0$), when the anti-plate shear waves act on the two holes with different parameters ka and d/a at the same time. In Fig. 2 (with holes spacing $d = 2.5$), analyzing the dynamic stress concentration around double holes, it can be seen that the value (2.06) at $\theta = \pi/2$ is much greater than the value (1.23) at $\theta = 3\pi/2$. In Fig. 3 (with holes spacing $d = 4.0$) analyzing the dynamic stress concentration around double holes, it can be seen that the value (1.87) at $\theta = \pi/2$ is slightly greater than the value (1.68) at $\theta = 3\pi/2$. Similar phenomena occur in Figs. 4 and 5, but due to the complicated effect resulted from the high wavenumber of incident wave, the variation trend is not so much obvious as Figs. 2 and 3.

Figs. 6–9 illuminate the hoop angular distributions of dynamic stress around the elliptic holes whose major axes go along with the x-direction in the infinite exponential graded materials with the non-homogeneous coefficient $\beta a = 0.2$ when the hole-spacing is $d/a = 2.5$ and $d/a = 4.0$ respectively. According to these curves, we can see that if the eccentricity ratio of elliptic hole is greater (for instance, $c = 1/6$), the mutual effect between two holes is more intensified, and the maximum of dynamic stress concentration is greater, especially when the wavenumber is high.

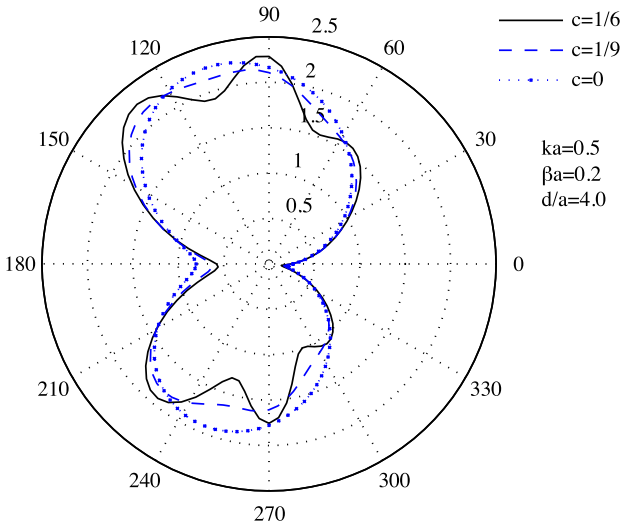

Fig. 8. Distributions of dynamic stress concentrations around two elliptic holes $ka = 0.5$, $\beta a = 0.2$, $d/a = 4.0$.

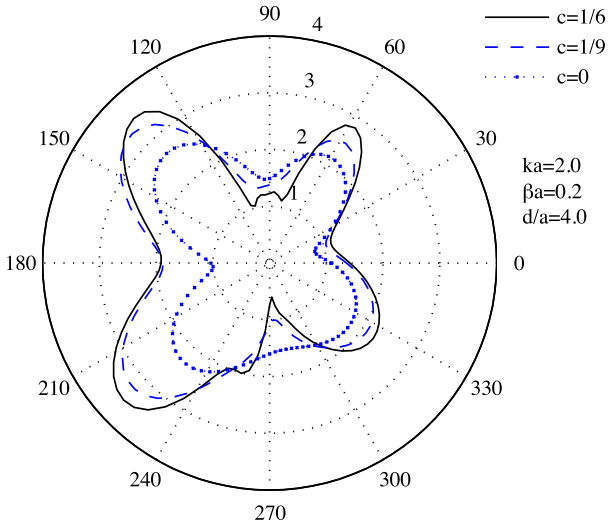

Fig. 9. Distributions of dynamic stress concentrations around two elliptic holes $ka = 2.0$, $\beta a = 0.2$, $d/a = 4.0$.

Figs. 10–11 describe the hoop angular distributions of dynamic stress around the elliptic holes whose major axes go along with the y direction in the infinite exponential graded materials with the non-homogeneous coefficient $\beta a = 0.2$. Compared with the case of circular hole, in this case the dynamic stress concentration has an obvious trend of shifting toward the illuminating side of the hole.

Shown in Fig. 12 is that the maximum of dynamic stress distributions around the elliptic holes (the eccentricity of holes $c = 1/6$) in the infinite exponential graded materials vary with the spacing between two holes, when the values of incident waves are different.

6. Conclusions

According to analyzing the numerical results above, the following conclusions are drawn:

1. Compared with the situation of a single hole, the variations of dynamic stress concentration factors for two elliptic holes are complex due to the influence of interaction between two holes. In most cases the dynamic stress concentrations are intensified, while sometimes are relieved.
2. Analyzing the dynamic stress concentration around double holes, for the upper hole, the value at $\theta = \pi/2$ is greater than the value at $\theta = 3\pi/2$. That is to mean: the mutual effect between two holes makes the dynamic stress of top half greater than bottom half.

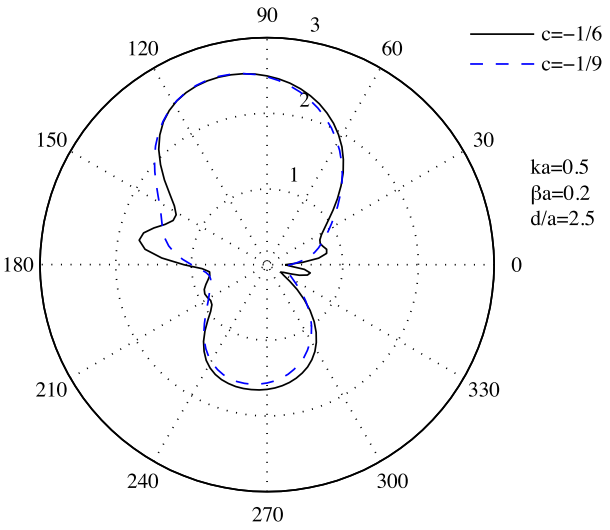

Fig. 10. Distributions of dynamic stress concentrations around two elliptic holes $ka = 0.5$, $\beta a = 0.2$, $d/a = 2.5$.

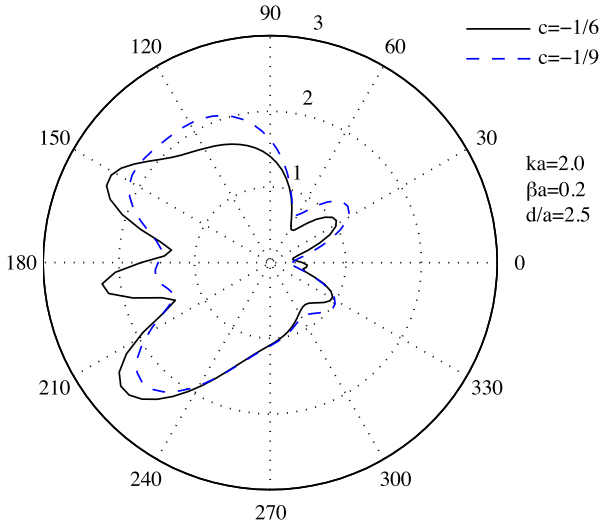

Fig. 11. Distributions of dynamic stress concentrations around two elliptic holes $ka = 2.0$, $\beta a = 0.2$, $d/a = 2.5$.

3. As the incident waves are at low frequency, minimum hole-spacing to ensure no mutual effect between holes is small; as the incident waves are at high frequency, minimum hole-spacing to ensure no mutual effect between holes is great.
4. The non-homogeneous coefficient of functional graded materials expresses great effect on the dynamic stress concentration around the holes. If the non-homogeneous parameter is greater than zero, that is to say, the material properties increase in the positive x-direction, the effect of the spacing between the two holes is greater.
5. If the eccentricity ratio of elliptic hole is greater (for instance, $c = 1/6$), the mutual effect between two holes is more intensified, and the maximum of dynamic stress concentration is greater, especially in the region of high wavenumber. When the eccentricity ratio of elliptic hole is less than zero, the maximum dynamic stress has an obvious trend of shifting toward the illuminating side of the hole.
6. Differing from static stress concentrations, with the increase of the spacing between two holes, dynamic stress concentrations around two holes increase at the beginning and then decrease. After that, a long oscillation process continues until an asymptotic value.

On the basis of the elastic wave scattering theory, we investigate the scattering of elastic wave and dynamic stress concentration problem in exponential graded materials with two holes. By using the complex function method and the local coordinate system, the solutions of this problem under the influence of incident waves with different wave numbers are obtained. And then by the orthogonal functions expansion method a solution of this problem can be reduced to the

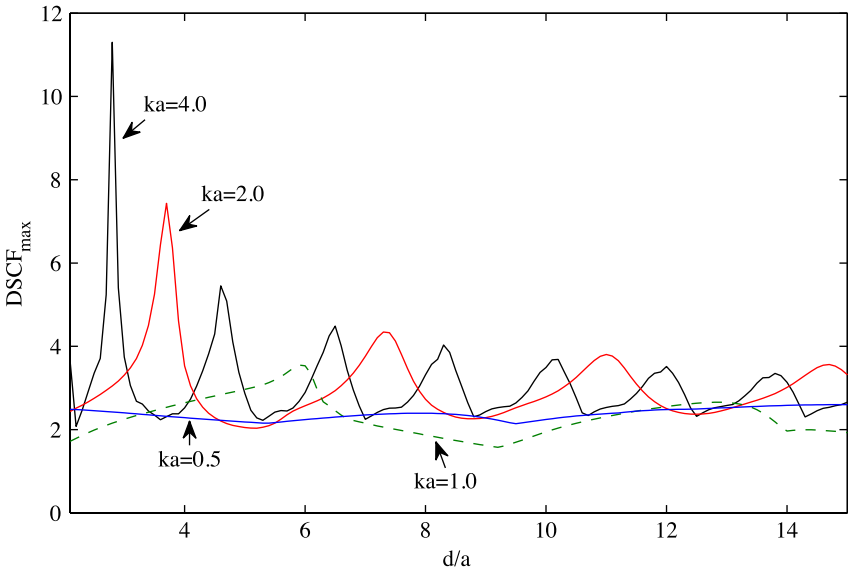

Fig. 12. Dynamic stress concentrations versus holes spacing ($c = 1/6$).

solution of an infinite system of algebraic equations. Also the numerical results of dynamic stress concentration factors around the two elliptic holes are given and discussed.

The theory and the numerical results in this paper can be taken as the theoretical basis and reference data for the dynamic analysis and strength design of the functional graded materials, the structural precision design and light weight design of structure.

Acknowledgment

This paper is supported by the National Natural Science Foundation of China (Foundation No. 10572045).

References

[1] Y.H. Pao, C.C. Maw, Diffraction of Elastic Wave and Dynamic Stress Concentration, Crane and Russak, New York, 1973.
[2] Y.H. Pao, Elastic wave in solids, J. Appl. Mech. 50 (4) (1983) 1152–1164.
[3] N.I. Muskhelishvili, Some Basic Problems of the Mathematical Theory of Elasticity, Springer, 1977.
[4] D.K. Liu, F. Han, Scattering of plane SH-wave by cylindrical canyon of arbitrary shape, Soil Dyn. Earthq. Eng. 10 (5) (1991) 249–255.
[5] C. Li, G.J. Weng, Dynamic stress intensity factor of a cylindrical interface crack with a functionally graded interlayer, Mech. Mater. 33 (2000) 325–333.
[6] S. Ueda, The surface crack problem for a layered plate with a functionally graded non-homogeneous interface, Int. J. Fract. 110 (2001) 189–204.
[7] X. Han, G. Liu, Elastic waves in a functionally graded piezoelectric cylinder, Smart Mater. Struct. 12 (6) (2003) 962–969.
[8] J. Chen, Z.X. Liu, Transient response of a mode III crack in an orthotropic functionally graded strip, Eur. J. Mech. A Solids 24 (2) (2005) 325–336.
[9] L. Ma, et al., Dynamic stress intensity factor for cracked functionally graded orthotropic medium under time-harmonic loading, Eur. J. Mech. A Solids 26 (2) (2007) 325–336.
[10] X.Q. Fang, C. Hu, S.Y. Du, Dynamic stress of a circular cavity buried in a semi-infinite functionally graded material subjected to shear waves, J. Appl. Mech. 74 (2007) 916–922.
[11] C.H. Daros, On modelling SH-waves in a class of inhomogeneous anisotropic media via the boundary element method, ZAMM Z. Angew. Math. Mech. 90 (2) (2010) 113–121.
[12] P.A. Martin, Scattering by defects in an exponentially graded layer and misuse of the method of images, Int. J. Solids Struct. 48 (14) (2011) 2164–2166.
[13] Q. Yang, C.-F. Gao, W.T. Chen, Stress analysis of a functional graded material plate with a circular hole, Arch. Appl. Mech. 80 (8) (2010) 895–907.
[14] Q. Yang, C.-F. Gao, Dynamic stress analysis of a functionally graded material plate with a circular hole, Meccanica 48 (1) (2013) 91–101.
[15] A. Bedford, D.S. Drumheller, Introduction to Elastic Wave Propagation, Wiley, 1994.
[16] A.S. Saada, Elasticity: Theory and Applications, J. Ross Pub., 2009.